4-5-2017

Development of BS-PT based high temperature ultrasonic transducer

Prathamesh N. Bilgunde
Iowa State University, pratham@iastate.edu

Leonard J. Bond
Iowa State University, bondlj@iastate.edu

Development of BS-PT based high temperature ultrasonic transducer

Abstract
High temperature (HT) environment in liquid metal cooled reactors poses major challenges towards development of ultrasonic transducer which is a key enabling technology for safety of reactors. In the current work, BS-PT (BiScO3- PbTiO3) piezoelectric material based ultrasonic transducer is proposed for the structural health monitoring at HT. Physics based model using finite element method simulates effect of temperature increase on the transduction ability of the BSPT piezoelectric material. Pulse-echo contact measurements are performed up to 260C which is the hot stand by temperature for liquid metal cooled reactors, to study the performance of the acoustic coupling agent and the BS-PT piezoelectric material bonded to a low-carbon steel sample. Experimental contact measurements indicate 6dB reduction in amplitude of the first backwall echo from 20C to 260C. Also, 0.1 MHz reduction in the fundamental and third harmonic resonance is observed in the spectral analysis of the first backwall echo.

Keywords
high temperature, piezoelectric, BS-PT, finite element, liquid metal, reactor, ultrasonic, transducer

Comments
This proceeding is published as Prathamesh Bilgunde, Leonard J. Bond, "Development of BS-PT based high temperature ultrasonic transducer," *Proc. SPIE* 10170, Health Monitoring of Structural and Biological Systems 2017, 1017014 (5 April 2017). doi: 10.1117/12.2260324. Posted with permission.

Development of BS-PT based high temperature ultrasonic transducer

Prathamesh Bilgunde, Leonard J. Bond

Prathamesh Bilgunde, Leonard J. Bond, "Development of BS-PT based high temperature ultrasonic transducer," Proc. SPIE 10170, Health Monitoring of Structural and Biological Systems 2017, 1017014 (5 April 2017); doi: 10.1117/12.2260324

SPIE.

Event: SPIE Smart Structures and Materials + Nondestructive Evaluation and Health Monitoring, 2017, Portland, Oregon, United States

Development of BS-PT based High Temperature Ultrasonic transducer

Prathamesh Bilgunde*[a], Leonard J. Bond[a]
[a] Department of Aerospace Engineering, Iowa State University, Ames, IA-50011

ABSTRACT

High temperature (HT) environment in liquid metal cooled reactors poses major challenges towards development of ultrasonic transducer which is a key enabling technology for safety of reactors. In the current work, BS-PT ($BiScO_3$-$PbTiO_3$) piezoelectric material based ultrasonic transducer is proposed for the structural health monitoring at HT. Physics based model using finite element method simulates effect of temperature increase on the transduction ability of the BSPT piezoelectric material. Pulse-echo contact measurements are performed up to 260C which is the hot stand by temperature for liquid metal cooled reactors, to study the performance of the acoustic coupling agent and the BS-PT piezoelectric material bonded to a low-carbon steel sample. Experimental contact measurements indicate 6dB reduction in amplitude of the first backwall echo from 20C to 260C. Also, 0.1 MHz reduction in the fundamental and third harmonic resonance is observed in the spectral analysis of the first backwall echo.

Keywords: high temperature, piezoelectric, BS-PT, finite element, liquid metal, reactor, ultrasonic, transducer

1. INTRODUCTION

The applications of ultrasonic transducers in high temperature and harsh environment is expanding rapidly in nuclear power industry, gas turbines and the space exploration technology [1-9]. These electro-mechanical sensors play an important role in the performance efficiency and life extension of critical infrastructure by providing a structural health insight through an ultrasonic scan [1][8][9]. During the past 40 years, extensive experimental work on high temperature (HT) ultrasonic transducer has been reported, but many transducers demonstrated limits to performance and life [9]. The monitoring of the transducer performance has been limited to measurement of d_{33} of the piezoelectric material as a function of temperature [7].

However, characteristics of temperature dependence of the full-material property matrix of piezoelectric ceramics has been reported in the past [10-19] which needs to be utilized to quantify the performance of HT piezoelectric transducers. Eitel et al. [14] first reported the (1-x) $BiScO_3$-x$PbTiO_3$ at its morphotropic phase boundary (MPB) (x=0.64) as a promising candidate for high temperature applications because of its relatively high piezoelectric response as compared to PZT-5A. Moreover, it has a high Curie temperature due to the small Perovskite tolerance factor of $BiScO_3$ in the solid-solution system with $PbTiO_3$ [15]. Gotmare et al. [16], [17] reported the thermal degradation and aging of BS-PT material with MPB and tetragonal compositions. Recently, Li et al. [20] used BS-PT material for high temperature structural health monitoring applications.

The need of computer of simulations to predict performance of a HT electro-mechanical device was reported by Tang et al. [13]. In 2014, Roy et al. [21] developed temperature dependent, physics based model using experimental data until 80 C. The objective of this work [21] was to propose a temperature compensation strategy for guided waves.

Acoustic coupling for the high temperature ultrasonic measurement is one of the critical challenges [6] for ultrasonic measurements at elevated temperature. It has been stated in previous study that 60% of high temperature transducers have adhesion problems [6]. Thus, it becomes necessary to understand and to select adhesives and bonding techniques which can provide bond-line integrity at high temperature.

Current work demonstrates temperature dependence of BSPT piezoelectric material and acoustic coupling, with physics based model data and pulse-echo contact measurements up to 260 C. Axisymmetric solution for the temperature dependent dynamic response of BSPT piezoelectric material disc is reported until 300 C. The physics based model is developed using finite element method in COMSOL software. This paper is divided into 4 sections. Section 2 presents fundamental theory regarding temperature dependence of piezoelectric material. Section 3 describes governing equations and boundary conditions for the predictive modeling of temperature effect on dynamic response of BSPT piezoelectric material. Section 4 reports experimental set-up and results of pulse echo contact measurements with spectral analysis of the data.

Health Monitoring of Structural and Biological Systems 2017, edited by Tribikram Kundu, Proc. of SPIE
Vol. 10170, 1017014 · © 2017 SPIE · CCC code: 0277-786X/17/$18 · doi: 10.1117/12.2260324

2. TEMPERATURE DEPENDENCE OF PIEZOELECTRIC MATERIAL

The strain charge form of linear theory of the piezoelectric effect can be given by [22]

$$S_i = s_{ij}^{\ E} T_j + d_{mi} E_m \tag{1}$$

$$D_m = d_{mi} T_i + \varepsilon_{mk}^{\ T} E_k \tag{2}$$

Where S_i is the total mechanical strain, D is the electric displacement, ε_{mk}^{T} is the absolute permittivity at constant mechanical stress T , $s_{ij}^{\ E}$ is the elastic compliance coefficient at a constant electric field E, and d_{mi} is the piezoelectric charge coefficient. The piezoelectric ceramic considered in this model is BSPT for which equation (1-2) can be represented in matrix form by

$$\begin{bmatrix} S1 \\ S2 \\ S3 \\ S4 \\ S5 \\ S6 \\ D1 \\ D2 \\ D3 \end{bmatrix} = \begin{bmatrix} s_{11}^E & s_{12}^E & s_{13}^E & 0 & 0 & 0 & 0 & 0 & d_{31} \\ s_{12}^E & s_{11}^E & s_{13}^E & 0 & 0 & 0 & 0 & 0 & d_{31} \\ s_{13}^E & s_{13}^E & s_{33}^E & 0 & 0 & 0 & 0 & 0 & d_{33} \\ 0 & 0 & 0 & s_{55}^E & 0 & 0 & 0 & d_{15} & 0 \\ 0 & 0 & 0 & 0 & s_{55}^E & 0 & d_{15} & 0 & 0 \\ 0 & 0 & 0 & 0 & 0 & 2(s_{11}^E - s_{12}^E) & 0 & 0 & 0 \\ 0 & 0 & 0 & 0 & d_{15} & 0 & \varepsilon_{11}^T & 0 & 0 \\ 0 & 0 & 0 & d_{15} & 0 & 0 & 0 & \varepsilon_{11}^T & 0 \\ d_{31} & d_{31} & d_{33} & 0 & 0 & 0 & 0 & 0 & \varepsilon_{33}^T \end{bmatrix} \begin{bmatrix} T_1 \\ T_2 \\ T_3 \\ T_4 \\ T_5 \\ T_6 \\ E_1 \\ E_2 \\ E_3 \end{bmatrix} \tag{3}$$

Due to the C∞/ C_{6v} symmetry and polarization of BSPT, the complete material matrix reduces to the five elastic, three piezoelectric and two dielectric coefficients as shown in equation (3). Thus, the temperature dependent data [18-19] for these ten coefficients completely describe the linear theory for the piezoelectric effect under the assumptions that—a) the piezoelectric material remains linearly elastic, and b) the applied electric field and mechanical stress are small which thus implies that this theory is not applicable for large deformations of the piezoelectric material. Sherrit et al. [23] have shown that

$$s_{lk}^{\ E} = s_{lk}^{'E}(\omega, E_i, T_j, T, t) + i\, s_{lk}^{''E}(\omega, E_i, T_j, T, t) \tag{4}$$

$$d_{ij} = d_{ij}^{'}(\omega, E_i, T_j, T, t) + i\ d_{ij}^{''}(\omega, E_i, T_j, T, t) \tag{5}$$

$$\varepsilon_{ij} = \varepsilon_{ij}^{'}(\omega, E_i, T_j, T, t) + i\ \varepsilon_{ij}^{''}(\omega, E_i, T_j, T, t) \tag{6}$$

Equation (4-6) shows s_{lk}^{E}, $d_{ij,}$ ε_{ij} are functions of angular frequency ω, applied mechanical stress T_j, temperature T and time t. The current work considers only the temperature dependency of the elastic, piezoelectric and dielectric coefficients for the finite element model. If the frequency dependent, and electric field dependent data is available, it can be fitted with a polynomial function of the dependent variables to give corresponding values for the material coefficients. From equations (1) to (6), the temperature dependent piezoelectric response function can be given by:

$$a(t) = f[S_{11}^{\ E}(T), S_{12}^{\ E}(T), S_{13}^{\ E}(T), S_{33}^{\ E}(T), S_{55}^{\ E}(T), d_{15}(T), d_{31}(T), d_{33}(T), \varepsilon_{11}(T), \varepsilon_{33}(T)] \tag{7}$$

To model equation (7), a physics based model is formulated in COMSOL using Lagrangian formulation. Reduction in the computational size is achieved by the assumption of the displacement field to be symmetric over an axis passing through center of the piezoelectric disc. Further details on modeling of dynamic response of piezoelectric material are discussed in the next section. Hence, current approach considers temperature dependency of ten material coefficients given by equation (7) instead of only d_{33} which was reported previously [7] to quantify performance of HT piezoelectric transducer.

3. PREDICTIVE MODELING METHODOLOGY

3.1 Frequency domain finite element (FDFE) approach

Using time domain finite element techniques, electrical impedance of a piezoelectric material can be computed from transient data of output voltage and current. Using fast Fourier transform, dynamic response of electrical impedance can then be plotted. However, wave-propagation study in time domain are computationally costly and require convergence study to set time step and the maximum element size. FDFE approach is basically a pseudo-static problem that requires no time stepping [24]. In current work FDFE approach is used to simulate temperature dynamic response of piezoelectric material. The geometric configuration of the problem is given by Fig.1

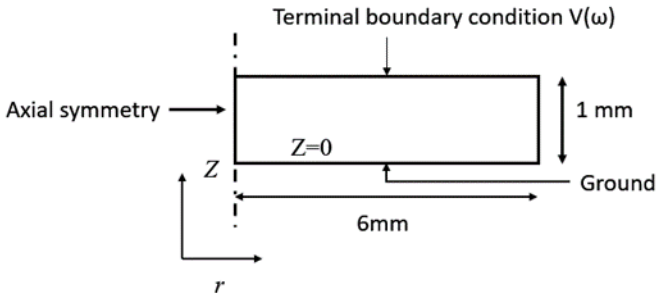

Figure 1-Geometric configuration of the problem

3.2 Linear momentum balance for piezoelectric material in frequency domain

The direct and converse piezoelectric effect are modelled using equation (1) and (2) respectively from section 2. The mechanical displacement field $u(r,\emptyset,z)$ is symmetric about axis Z. FDFE approach assumes time harmonic nature of displacement $u=u(r,\emptyset,z)\, e^{iwt}$ and stress $\sigma=\sigma(r,\emptyset,z)e^{iwt}$ in the cylindrical space co-ordinate system. The e^{iwt} describes the harmonic nature of the variable. Thus, the equation of linear momentum balance in the frequency domain is given by

$$\rho\omega^2 u + \nabla\bullet\sigma = F_v e^{i\phi} \tag{8}$$

Where ρ is the assigned material density, ω is the circular frequency for frequency sweep, F_v is the body force. Poling axis of BSPT is aligned with z axis of the model. Z=0 and Z=1 surfaces, shown in Fig. 1 are kept traction free ($\sigma_{zx}=\sigma_{zz}=\sigma_{xx}=0$).

3.3 Electrostatics

For the piezoelectric material, as stated previously electric field is assumed irrotational. Thus electric field E is related to the scalar electric potential V given as

$$E = -\nabla V \tag{9}$$

$$n\bullet D = 0 \tag{10}$$

Zero charge constraint is assigned in the domain Ω_{piezo} at boundaries x=0 and x=3. Charge density ρ_v in the domain Ω_{piezo} is given by

$$\nabla\bullet D = \rho_v \tag{11}$$

3.4 External electrical Circuit for the instrumentation impedance

In the experimental resonance measurements, piezo-electric is generally connected to impedance analyzer via lead wires soldered on the metal electrodes. This introduces potential electrical impedance mismatch between the piezo and the impedance analyzer. This is modelled by introducing a resistor of impedance equal to the impedance analyzer. In the current study, the impedance value of resistor is set to an ideal 50 Ω between node 1 and 2. The electric circuit module in COMSOL evaluates global variable voltage as a function of frequency sweep. In this model, AC voltage of amplitude 1V is applied to the piezoelectric material via external current coupling of the terminal boundary condition assigned to PZT shown in Fig.1.

The current on the piezoelectric electrode surface $\partial^D\Omega_{piezo}$ is

$$\int_{\partial^D\Omega_{piezo}} D \bullet n = Q_0, \frac{dQ_0}{dt} = I_{cir} \tag{12}$$

Hence the voltage on the electrode surface $\partial^D\Omega_{piezo}$ is given by

$$V_{pz}(\omega) = V_{source}(\omega) - I_{cir} R \tag{13}$$

Using the frequency dependent voltage and current, the electrical admittance can be plotted as a function of frequency.

3.5 Discretization

Quadrilateral element of size 0.01mm was used for mapped meshing of the complete domain Ω_{piezo}. Total number of elements are 32000 with average growth rate and average element quality equal to 1.

$$h_{\max} = \frac{c}{f_0 N} \tag{14}$$

Where h_{max} is the maximum element size, c is the shear wave speed in the piezoelectric material, f_0 is the highest frequency in the desired spectrum, N is the number of element per wavelength. Frequency step for the sweep is set to 1/500 of the largest frequency in the sweep. This increases number of sample points in the impedance spectra improving the resolution of the simulated data.

3.6 Model results

Ferroelectric ceramics exhibit both intrinsic and extrinsic contributions to the piezoelectric effect [25]. This effect given by equation (1-2) is dependent on the elastic, dielectric, and piezoelectric coefficients. Hence, the magnitude of these coefficients is dependent on the extrinsic and intrinsic properties of the ceramics [26]. In the FDFE approach electrical admittance, capacitance and electric charge are evaluated to quantify the temperature dependence of intrinsic and extrinsic contribution to the piezoelectric effect. The current physics based model applies the temperature dependent experimental data of the BSPT material given by Chen et al. [18] in the morphotropic phase boundary condition(MPB). The MPB is an almost-temperature-independent phase boundary that separates tetragonal crystal structure (P4mm) and a rhombohedral structure (R3c) [27]. Material sweep is performed in COMSOL to change the material matrix of the BSPT material corresponding to the predefined temperature. Fig.2(a-b) shows the temperature dependent dynamic response of real and imaginary part of electrical admittance.

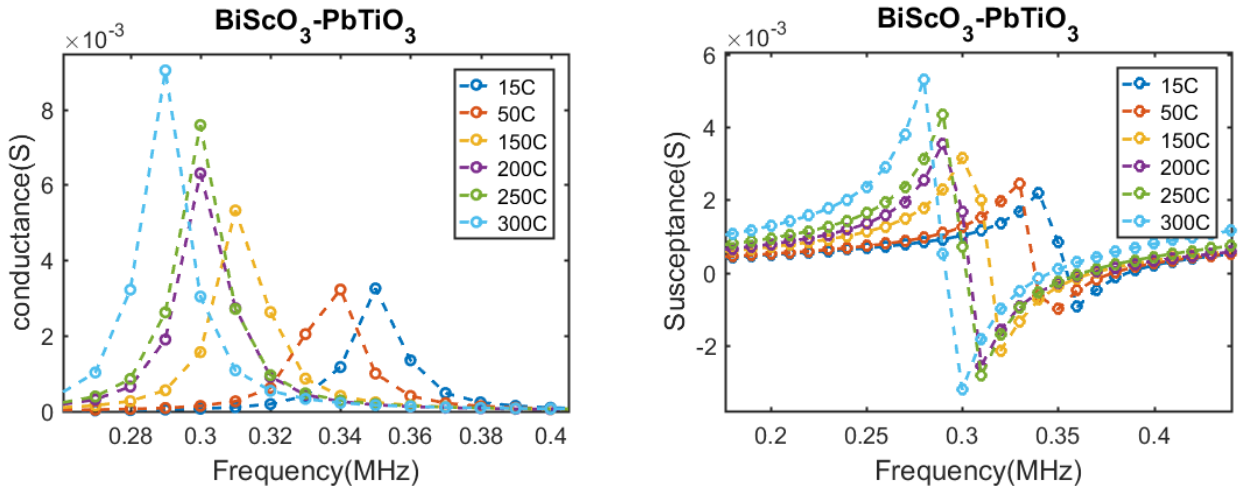

Figure 2 Dynamic response of a) conductance b) susceptance due to temperature dependent piezoelectric material matrix

As shown in Fig.2(a), the temperature increase of the piezoelectric material, increases the conductance of the material. It increases by a factor of 2.7 at 300C as compared to 15C. Fig.2(b) shows increase in the susceptance as a function of temperature. Admittance is a reciprocal of electrical impedance. This indicates, as the temperature increases, it decreases electrical impedance of the BSPT material. The spontaneous polarization P of the piezoelectric material is related to electric field E and electric displacement D given by

$$D_m = \varepsilon_0 E_m + P_m \tag{15}$$

$$P_m = \varepsilon_0 (\varepsilon_r - I) E_m + e\varepsilon \tag{16}$$

$$P_m = \varepsilon_0 \chi E_m + e\varepsilon \tag{17}$$

Where χ represents the dielectric susceptibility of the piezoelectric material. Fig.3(a) shows the experimental data on temperature dependence of dielectric constant of the BSPT piezoelectric ceramic disc as a function of frequency and temperature. The dielectric constant increases with temperature indicating increase in the dielectric susceptibility which can be understood from equation (16-17). Capacitance of the piezoelectric disc is directly proportional to dielectric constant for a constant area and thickness of the disc. Thus, from equation (16-17) and experimental data in Fig. 3(a), increase in dielectric susceptance due to temperature increase should increase the capacitance of the BSPT disc.

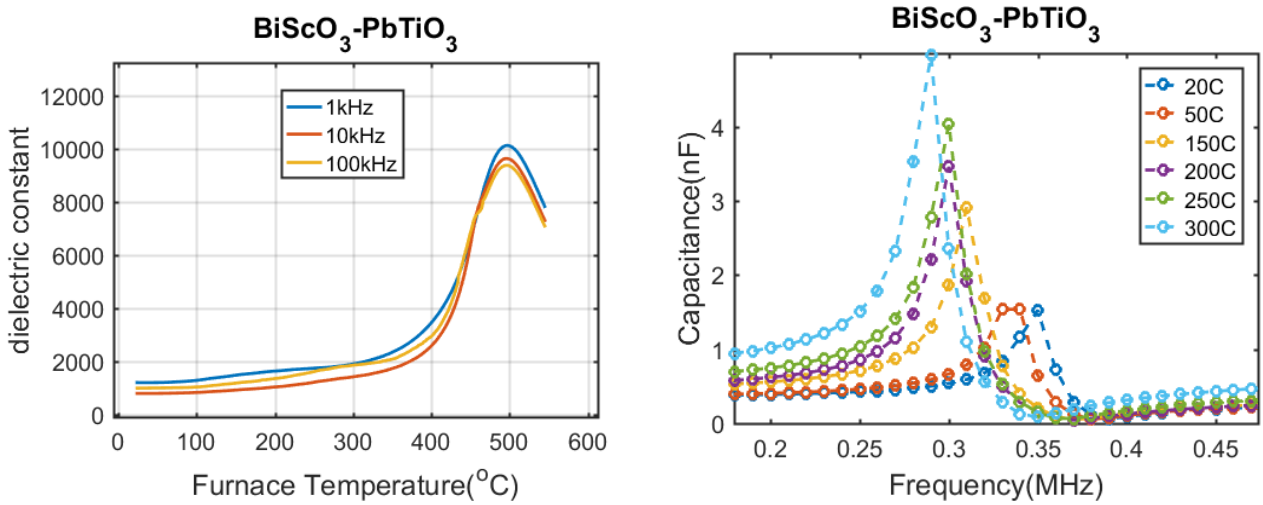

Figure 3- Temperature dependent a) Experimental data of dielectric constant b) Capacitance (Simulation data)

Predictive model developed using FDFE approach estimates this increase in the capacitance of BSPT disc as a function of temperature shown by Fig.3(b). The simulated data shows increase in the capacitance magnitude from 15C to 300C by a factor of 2.2. Increase in the capacitive ability of the dielectric indicates increased ability of storing electric charge. From the previous discussion, this implies that the increase in the temperature will increase the electric charge stored by the piezoelectric material. Fig.4 shows increase in the electric charge computed for BSPT from 15C to 300 C.

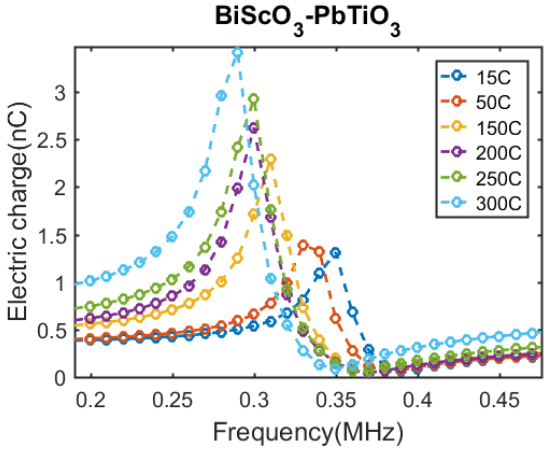

Figure 4- Simulation data for dynamic response of BSPT for temperature dependence of electric charge

4. HT PULSE-ECHO CONTACT MEASUREMENTS

4.1 Experimental Set-up preparation

Fig. 5 shows the schematic of the experimental set-up for the high temperature pulse-echo contact measurements. The thickness of BSPT material is 0.9mm and diameter is 0.75 inch. 0.008-inch diameter nickel lead wire is connected to the top electrode of BSPT using Duralco 124 [28]-a silver based conductive two components epoxy paste. The bond is cured in oven at 120 C for two hours with post cure heating of the bond for additional two hours at the same temperature. The conductivity is tested using electrical continuity mode on the digital multimeter. The ground connection is established by using Pyroduct-597A [29-30] which connects the nickel wire to a 0.5-inch-thick, cold drawn low-carbon steel block. The bond is cured at 120C for two hours. High temperature alumina ceramic tube is used as insulation for the nickel lead wires. The critical challenge of the experiment is acoustic coupling between the BSPT and carbon steel block. A two-part epoxy (Epotek 353ND) is used as a coupling agent for high temperature. The maximum rated temperature of Epotek 353ND for continuous operation is 250 C and 350 C for intermittent operation. The bond using Epotek 353ND is cured at 150C for one hour in the oven. Alumina ceramic tubes acts as insulation for the nickel wires to prevent electrical short.

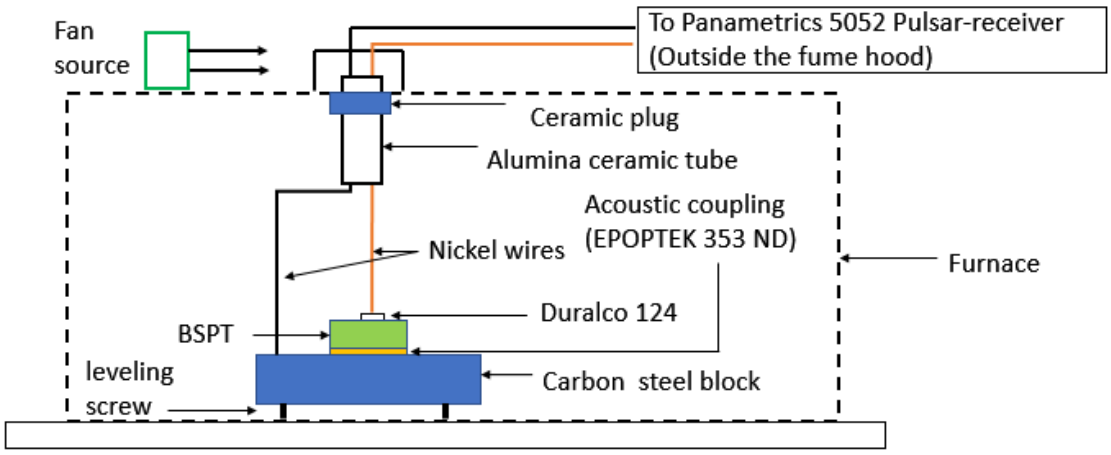

Figure 5-Schematic of the Experimental set-up for high temperature Pulse echo contact measurements

Fig. 6 shows the simplified diagram for the pulsar receiver(P-R) circuit [31]. The transmitted and received pulse data acquired from the transducer is dependent upon the energy, damping gain and filter settings of the P-R. In the current experimental set-up Panametrics 5052x P-R is used to excite the transducer with a spike of 100V (energy setting). The damping resistance (R_d) is adjusted to 50Ω. Gain setting is set to 16dB and high pass filter is adjusted to *out* setting. The rep. rate is set at 4. The pulse-echo data from the transducer is acquired using LeCroy HDO 4034 oscilloscope with a 12-bit resolution. The data is sampled at 450MHz with 512 times averaging to filter random electrical noise.

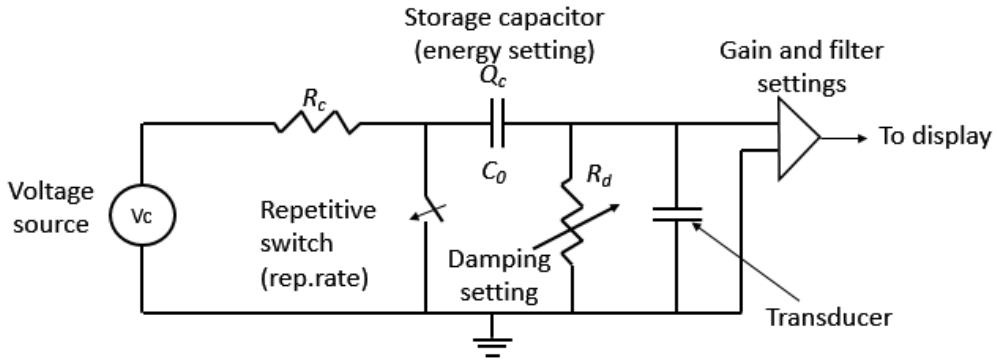

Figure 6-Simpliefied diagram of pulsar -receiver (recreated from [31])

4.2 In-oven pulse-echo measurements of BSPT attached to the 1018 low carbon steel block

The high temperature pulse-echo contact measurements are performed in Barnstead Thermolyne furnace type 47900. The set point of the furnace is defined as 260 C. Temperature is increased from 20 C at 5 C/min rate. The hold (dwell) time at 260C is set for 20 minutes. The P-R settings are not modified during the contact measurements. The averaged waveform is saved in HDO 4034 at every 10C increase in the furnace temperature.

Fig. 7(a) shows temperature effect on the averaged waveform representing the first backwall echo from the carbon steel block. It can be seen that the arrival time of the first backwall echo increases due to the acoustic impedance change of BSPT, acoustic coupling and the steel block.

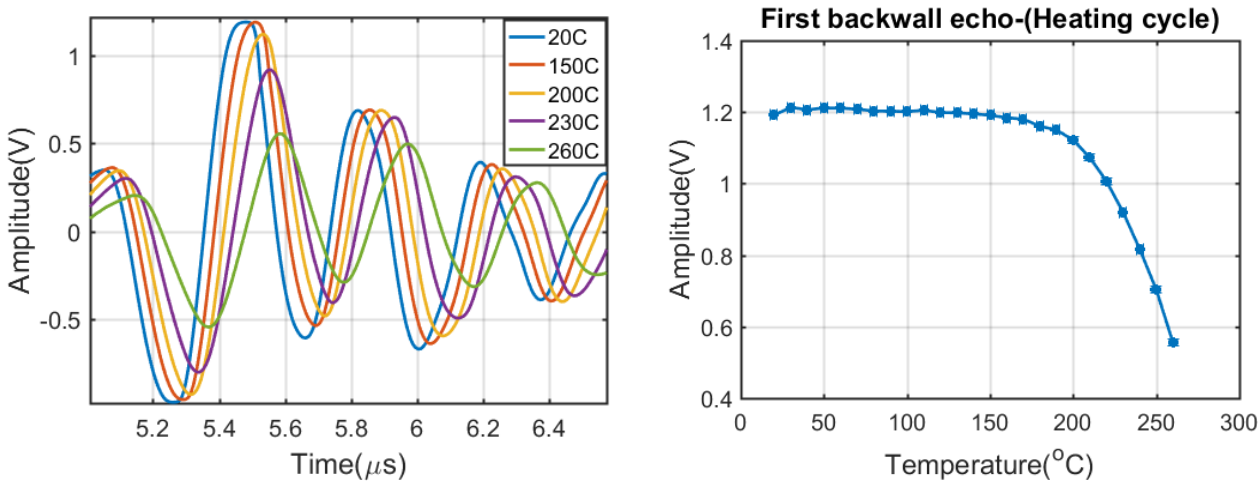

Figure 7-First back wall echo a) time domain signals b) amplitude as a function temperature

Fig.7(b) shows reduction in the amplitude of the first backwall echo as the temperature is increased from 20 C to 260C for the heating cycle. 6dB reduction in the amplitude is observed from 20C to 260C. The rate of reduction in the amplitude increases considerably after 200 C. Fig. 8(a-b) shows temperature effect on the spectral content of the first backwall echo.

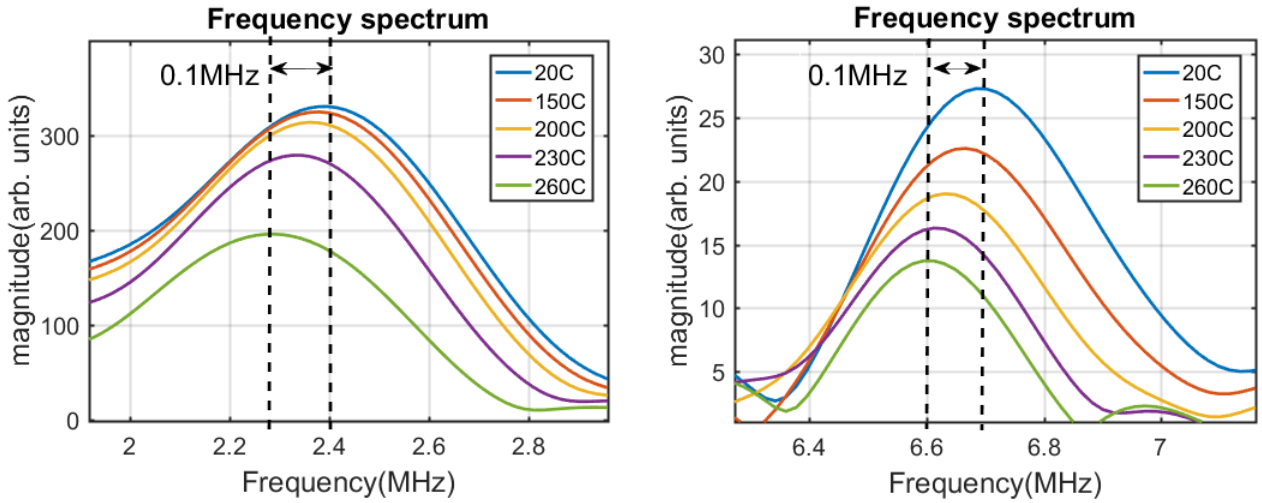

Figure 8-Temperature effect on a) Fundamental frequency resonance b) partial third harmonic resonance

Fig. 8(a) shows left shift of 0.1 MHz at 260C from the fundamental resonance frequency of the structure at 20C. Similarly, 0.1 MHz left shift is observed for the partial third harmonic of the structure at 260C.

5. SUMMARY AND CONCLUSION

The transduction ability of a piezoelectric material is represented by the piezoelectric effect. Ferroelectric ceramics exhibit both intrinsic and extrinsic contributions to this effect. In this work, predictive model is developed using frequency domain finite element (FDFE) approach which evaluates electrical admittance, capacitance and electric charge to quantify the temperature dependence of intrinsic and extrinsic contribution to the piezoelectric effect. The model considers temperature dependency of ten material coefficients instead of only d_{33} coefficient. Temperature increase from 15C to 300C estimates increase in the conductance and susceptance of BSPT material. The simulated data for increase in capacitance due to temperature increase, agrees with the experimental data which shows increase in dielectric constant. Increased capacitance consequently increases electric charge from 15C to 300C in the model.

High temperature pulse-echo contact measurements are performed up to 260C which is the hot stand by temperature for liquid metal cooled reactors, to study the performance of the acoustic coupling agent and the BS-PT piezoelectric material bonded to a low-carbon steel specimen. Experimental measurements indicate 6dB reduction in amplitude of the first backwall echo for contact measurement from 20C to 260C. Significant reduction in the amplitude occurred from 200C to 260C. Also, 0.1 MHz reduction in the spectral content of the first backwall echo is observed. This could be due to temperature dependent acoustic impedance of BSPT, acoustic coupling (Epotek 353ND) and the low-carbon steel.

In the experimental approach, it is challenging to decouple the temperature effect of BSPT, acoustic coupling and the low carbon steel. Hence, current predictive model will be extended to the experimental set-up for further investigation of significant reduction in backwall echo amplitude from 200C to 260C. The hypothesis is that the significant change in the acoustic impedance of acoustic coupling, Epotek 353ND causes attenuation of the reflected signal from the bottom surface of low carbon steel block in the temperature range 200C to 260C.

ACKNOWLEDGEMENT

This work is funded by the U.S. Department of Energy's office of Nuclear Energy under Nuclear Energy University programs (NEUP) under contract DE-NE0000676 and performed at Center for NDE, Iowa State University. The authors would like to thank Kathleen Wilcox and Prof. Xiaoli Tan (Department of Material Science and Engineering, Iowa State University) for performing dielectric constant measurements of BSPT material as shown in Fig. 3. The authors would also like to thank Daniel Barnard (Center for NDE) for helping with the experimental set-up for high temperature contact measurements and also for useful discussions.

REFERENCES

[1] Searfass, C. T., Pheil, C., Sinding, K., Tittmann, B. R., Baba, A., and Agrawal, D. K., "Bismuth Titanate Fabricated by Spray-on Deposition and Microwave Sintering for High-Temperature Ultrasonic Transducers". *IEEE transactions on Ultrasonics, Ferroelectrics, and Frequency control*, *63*(1), 139-146. (2016).

[2] Bar-Cohen, Y. [High Temperature Materials and Mechanisms] CRC Press: Boca Raton, FL, USA, pp. 487, (2014)

[3] Bar-Cohen, Y., Bao, X., Badescu, M., Sherrit, S., Lee, H.J., Zacny, K., Kumar, N. and Mumm, E., Drilling and Sample Transfer Mechanisms for Potential Missions to Venus. In *Inner Solar System* (pp. 163-187). Springer International Publishing. (2015)

[4] Lee, H. J., Zhang, S., Bar-Cohen, Y., and Sherrit, S. "High temperature, high power piezoelectric composite transducers". *Sensors*, *14*(8), 14526-14552. (2014)

[5] Parks, D. A., Zhang, S., and Tittmann, B. R. "High-temperature (> 500/spl deg C) ultrasonic transducers: an experimental comparison among three candidate piezoelectric materials". *IEEE transactions on Ultrasonics, Ferroelectrics, and Frequency control*, *60*(5), 1010-1015. (2013).

[6] Kažys, R., Voleišis, A., and Voleišienė, B. "High temperature ultrasonic transducers: review". *Ultragarsas Ultrasound*, *63*(2), 7-17. (2008).

[7] D. A. Parks and B. R. Tittmann, "Ultrasonic NDE in a reactor core",*2011 IEEE SENSORS Proceedings*, Limerick, pp.618-622. (2011) doi: 10.1109/ICSENS.2011.6126944

[8] Augereau, F. P., Ferrandis, J. Y., Villard, J. F., Fourmentel, D., Dierckx, M., and Wagemans, J., "Effect of intense neutron dose radiation on piezoceramics", *Journal of the Acoustical Society of America*, *123(*5), 3928. (2008).

[9] Griffin, J. W., Peters, T. J., Posakony, G. J., Chien, H. T., Bond, L. J., Denslow, K. M., Sheen, S. H. and Raptis, P. "Under-Sodium viewing: a review of ultrasonic imaging technology for liquid metal fast reactors," PNNL-18292, Pacific Northwest National Laboratory, Richland, WA (2009).

[10] Georges Sabat, R., Mukherjee, B. K., Ren, W., and Yang, G. "Temperature dependence of the complete material coefficients matrix of soft and hard doped piezoelectric lead zirconate titanate ceramics". *Journal of Applied Physics*, *101*(6), 064111. (2007).
[11] Kim, T., Kim, J., Dalmau, R., Schlesser, R., Preble, E., and Jiang, X. "High-temperature electromechanical characterization of AlN single crystals". *IEEE transactions on Ultrasonics, Ferroelectrics, and Frequency control*, *62*(10), 1880-1887. (2015).
[12] Hooker M. W., "Properties of pzt-based piezoelectric ceramics between-150 and 250c," NASA/CR-1998-208708, National Aeronautics and Space Administration, Langley Research Center (1998).
[13] Tang, L., and Cao, W. "Temperature dependence of self-consistent full matrix material constants of lead zirconate titanate ceramics". *Applied Physics Letters*, *106*(5), 052902. (2015)
[14] Eitel, R. E., Randall, C. A., Shrout, T. R., Rehrig, P. W., Hackenberger, W., and Park, S. E. "New high temperature morphotropic phase boundary piezoelectrics based on Bi (Me) O3–PbTiO3 ceramics." *Japanese Journal of Applied Physics*, *40*(10R), 5999. (2001).
[15] Eitel, R. E., Randall, C. A., Shrout, T. R., and Park, S. E. "Preparation and characterization of high temperature perovskite ferroelectrics in the solid-solution (1-x) BiScO3–xPbTiO3". *Japanese Journal of Applied Physics*,*41*(4R), 2099. (2002)
[16] Gotmare, S. W., Leontsev, S. O., and Eitel, R. E. "Thermal Degradation and Aging of High-Temperature Piezoelctric Ceramics". *Journal of the American Ceramic Society*, *93*(7), 1965-1969. (2010).
[17] Gotmare, Sunil W., "Thermal Degradation and Aging of High Temperature Piezoelectric Ceramics" (2008). University of Kentucky Master's Theses. paper564. http://uknowledge.uky.edu/gradschool_theses/564
[18] Chen, J., Shi, H., Liu, G., Cheng, J., and Dong, S. "Temperature dependence of dielectric, piezoelectric and elastic properties of BiScO 3–PbTiO 3 high temperature ceramics with morphotropic phase boundary (MPB) composition". *Journal of Alloys and Compounds*, *537*, 280-285. (2012).
[19] Chen, J., Cheng, J., and Dong, S. "Review on high temperature piezoelectric ceramics and actuators based on BiScO 3–PbTiO 3 solid solutions". *Journal of Advanced Dielectrics*, *4*(01), 1430002. (2014).
[20] Li Y. H., Kim, S. J., Salowitz, N., and Chang, F. K, "Development of High-Performance BS-PT Based Piezoelectric Transducers for High-Temperature Applications". *In EWSHM-7th European Workshop on Structural Health Monitoring*. (2014)
[21] Roy, S., Lonkar, K., Janapati, V., and Chang, F. K., "A novel physics-based temperature compensation model for structural health monitoring using ultrasonic guided waves". *Structural Health Monitoring*, *13*(3), 321-342. (2014).
[22] Jaffe, B., Cook, Jr., W. R., and Jaffe, H., [Piezoelectric ceramics](Academic Press, London) (1971).
[23] Sherrit, S., and Mukherjee, B. K. "Characterization of Piezoelectric Materials for Transducers", Dielectric and Ferroelectric Reviews, 175-244, ISBN: 978-81-308-0378-4, Editors: Srowthi S. N. Bharadwaja and Robert A Dorey, previously published on Arxiv. (2012) http://arxiv.org/ftp/arxiv/papers/0711/0711.2657.pdf
[24] Chillara, V. K., Ren, B., and Lissenden, C. J. "Guided wave mode selection for inhomogeneous elastic waveguides using frequency domain finite element approach". *Ultrasonics*, 67, 199-211. (2016).
[25] Li, S., Cao, W., and Cross, L. E. "The extrinsic nature of nonlinear behavior observed in lead zirconate titanate ferroelectric ceramic". *Journal of Applied Physics*, *69*(10), 7219-7224. (1991).
[26] Randall, C. A., Kim, N., Kucera, J. P., Cao, W., and Shrout, T. R. "Intrinsic and extrinsic size effects in fine-grained morphotropic-phase-boundary lead zirconate titanate ceramics". *Journal of the American Ceramic Society*, *81*(3), 677-688. (1998).
[27] Haun, M. J., Furman, E., Jang, S. J., McKinstry, H. A., and Cross, L. E. "Thermodynamic theory of PbTiO3" *Journal of Applied Physics*, *62*(8), 3331-3338. (1987).
[28] Dhutti, A., Tumin, S. A., Mohimi, A., Kostan, M., Gan, T. H., Balachandran, W., and Selcuk, C. "Development of Low Frequency High Temperature Ultrasonic Transducers for In-service Monitoring of Pipework in Power Plants". *Procedia Engineering*, *168*, 983-986. (2016).
[29] Giurgiutiu, V., Xu, B., and Liu, W. "Development and testing of high-temperature piezoelectric wafer active sensors for extreme environments". *Structural Health Monitoring*,*9*(6),513-525 (2010).
[30] Amini, M. H., Sinclair, A. N., and Coyle, T. W. "A New High-Temperature Ultrasonic Transducer for Continuous Inspection". *IEEE transactions on Ultrasonics, Ferroelectrics, and Frequency control*, *63*(3), 448-455. (2016).
[31] Schmerr Jr. L. W., [Fundamentals of Ultrasonic Nondestructive Evaluation: A Modeling Approach,] (Plenum: New York), p.21, Springer (1998)